Simulation of field-induced structural formation and transition in electromagnetorheological suspensions

Zuowei Wang,* Haiping Fang, Zhifang Lin, and Luwei Zhou
Department of Physics, Fudan University, Shanghai 200433, People's Republic of China
(Received 17 June 1999)

A computer simulation method has been used to study the three-dimensional structural formation and transition of electromagnetorheological (EMR) suspensions under compatible electric and magnetic fields. When the fields are applied simultaneously and perpendicularly to each other, the particles rapidly arrange into single layer structures parallel to both fields. In each layer, there is a two-dimensional hexagonal lattice. The single layers then combine together to form thicker sheetlike structures. With the help of the thermal fluctuations, the thicker structures relax into three-dimensional close-packed structures, which may be face-centered cubic (fcc), hexagonal close-packed (hcp) lattices, or, more probably, the mixture of them, depending on the initial configurations and the thermal fluctuations. On the other hand, if the electric field is applied first to induce the body-centered tetragonal (bct) columns in the system, and then the magnetic field is applied in the perpendicular direction, the bct to fcc structure transition is observed in a very short time. Following that, the structure keeps on evolving due to the demagnetization effect and finally forms close-packed structures with fcc and hcp lattice character. The simulation results are in agreement with the theoretical and experimental results.

PACS number(s): 83.80.Gv, 61.90.+d, 61.20.Ja

I. INTRODUCTION

Electrorheological (ER) and magnetorheological (MR) fluids are typically comprised of polarizable particles dispersed in a liquid. When an electric or magnetic field is applied, the particles aggregate to form chain or column structures which modify the effective viscosities of the fluids dramatically. Though the ER and MR phenomena are similar in character, the fundamental physical mechanisms responsible for them are different. Each of them has characteristic advantages and disadvantages [1–4]. Recently, there have been some attempts to combine the ER and MR effects for getting better rheological properties. One attempt is the development of the electromagnetorheological (EMR) suspensions by using the materials responsive to both electric and magnetic fields as the dispersed phase [2–4]. Experiments showed that the shear stress induced in EMR suspensions by the combined electric and magnetic fields is larger than that expected from the linear additivity of the ER and MR effects. This synergistic EMR effect has been observed in both the parallel-field and crossed-field conditions, and it is significant in the parallel-field condition [3,4]. For understanding the mechanism of the synergistic EMR effect, it is necessary to clarify the structure change of the EMR suspensions under different field conditions.

When the electric and magnetic fields are applied in parallel, the structure change of the EMR suspensions is similar to that in ER and MR fluids. Chain or column structures are formed along the field direction with the body-centered tetragonal (bct) structure as their ground state. The obvious synergistic EMR effect in this case is assigned to the increase of the number of the chains bridging the plates [3]. However, when the fields are applied perpendicularly, the structure formed in EMR suspensions depends on the ratio between the strength of the fields. Theoretical calculations indicate that if the electric (or magnetic) field is dominant, the ideal structure of the system is still the bct lattice with its fourfold rotational axis along the dominant field [5,6]. When the ratio between the fields exceeds a minimum value so that the electric and magnetic interactions between the particles become compatible, the dipolar energy for the hexagonal close-packed (hcp) and face-centered cubic (fcc) lattices will be much smaller than that of the bct lattice, implying a structural transition from the bct lattice to the close-packed lattice [5,6]. Since the energy difference between the hcp and fcc structures is very small and compatible to the thermal energy at room temperature, the EMR system may develop into a hcp, a fcc, or, more likely, a mixed hcp-fcc structure under compatible fields [5]. The structural transition from bct to fcc had been observed in experiment where the electric field was applied first to induce bct columns in the suspension and the compatible magnetic field was then applied in the perpendicular direction [6]. The possibility for the formation of different lattice structures in EMR suspensions is also an interesting physical phenomenon worth investigating, because it has many potential applications, especially in manufacturing mesocrystals with unique photonic properties [6].

In this paper, we present the molecular dynamic simulation studies on the dynamic structural evolution of EMR suspensions. The studies are concentrated on the crossed-field condition, because most of the interesting structuring processes occur in this case. The compatible electric and magnetic fields are supposed to be applied in two orders. One is applying both fields simultaneously to the initial random configurations. The other is that the electric field is applied first so as to induce the bct columns in the suspensions, and

*Present address: Laboratoire de Physique de la Matière Condensée, Université de Nice–Sophia Antipolis, Parc Valrose, 06108 Nice Cedex 2, France. Electronic address: wang@unice.fr

the magnetic field is then applied in the perpendicular direction. In the former case, we find that the final structure of EMR suspensions under compatible fields is the mixed hcp-fcc structure, in good agreement with the theoretical predication [5]. The thermal fluctuation is found to play an important role in the formation of the lattice structures. In the latter case, the structural transition from bct to fcc is found shortly after the application of the magnetic field. The observed dynamic process of the structural transition is consistent with the theoretical explanation for the experimental results [6]. Following this transition, the structure keeps on evolving due to the demagnetization effect. The final state is also a mixed hcp-fcc structure. The details of the final structures are found to depend on the initial configurations, the thermal fluctuations, the field conditions, and the properties of the EMR materials in both cases.

II. SIMULATION METHOD

The EMR system studied in this paper is supposed to consist of spherical particles of uniform diameter σ, dielectric constant ϵ_p, and magnetic permittivity μ_p suspended in a nonconducting Newtonian fluid. The fluid has a viscosity η_f, dielectric constant ϵ_f, and magnetic permittivity μ_f with $\epsilon_p > \epsilon_f$ and $\mu_p > \mu_f$. The suspension can behave as both an ER fluid and a MR fluid. In practice, the dispersed phase can be ferromagnetic particles coated with an ER active layer or dielectric particles coated with a MR active layer [2–6].

When an electric field $\mathbf{E}_0$ is applied to the suspension, the electric dipole moment induced on a particle is [7,8]

$$\mathbf{p}_i = \pi \epsilon_0 \epsilon_f \alpha \sigma^3 \mathbf{E}_{\mathrm{loc}}/2, \tag{1}$$

$$\mathbf{E}_{\mathrm{loc}} = \mathbf{E}_0 + \sum_{j \neq i} \mathbf{E}_p^j, \tag{2}$$

$$\mathbf{E}_p^j = \frac{3(\mathbf{p}_j \cdot \mathbf{e}_r)\mathbf{e}_r - \mathbf{p}_j}{4\pi \epsilon_0 \epsilon_f r_{ij}^3}, \tag{3}$$

where $\mathbf{r}_{ij} = \mathbf{r}_i - \mathbf{r}_j$ and $\alpha = (\epsilon_p - \epsilon_f)/(\epsilon_p + 2\epsilon_f)$. $\mathbf{E}_{\mathrm{loc}}$ is the local electric field evaluated at the center of i, which is determined by the external field as well as the dipole fields from all other particles in the simulation cell and their periodic images within a cutoff radius of r_c. The electric static interaction force between two particles is given by

$$\mathbf{F}_{ij}^{\mathrm{el}}(\mathbf{r}_{ij}) = 3\frac{[3(\mathbf{p}_i \cdot \mathbf{e}_r)(\mathbf{p}_j \cdot \mathbf{e}_r) - \mathbf{p}_i \cdot \mathbf{p}_j]\mathbf{e}_r - [(\mathbf{p}_i \cdot \mathbf{e}_\theta)(\mathbf{p}_j \cdot \mathbf{e}_r) + (\mathbf{p}_i \cdot \mathbf{e}_r)(\mathbf{p}_j \cdot \mathbf{e}_\theta)]\mathbf{e}_\theta}{4\pi \epsilon_0 \epsilon_f r_{ij}^4}. \tag{4}$$

The scale of the electrostatic force can be evaluated from the parameter $F_0^{\mathrm{el}} = 3\pi \epsilon_0 \epsilon_f \alpha^2 \sigma^2 E_0^2/16$. Similarly, if the system is exposed to an external magnetic field $\mathbf{H}_0$, the induced magnetic dipole moment on a particle is

$$\mathbf{m}_i = \pi \mu_0 \mu_f \beta \sigma^3 \mathbf{H}_{\mathrm{loc}}/2, \tag{5}$$

where $\beta = (\mu_p - \mu_f)/(\mu_p + 2\mu_f)$. The calculation of the local magnetic field $\mathbf{H}_{\mathrm{loc}}$ and the magnetic static interaction force $\mathbf{F}_{ij}^{\mathrm{mag}}(\mathbf{r}_{ij})$ between two particles is analogous to that in the electric field. The scale of the magnetic force is evaluated by $F_0^{\mathrm{mag}} = 3\pi \mu_0 \mu_f \beta^2 \sigma^2 H_0^2/16$. The parameter $\xi = F_0^{\mathrm{mag}}/F_0^{\mathrm{el}}$ can be used to measure the competition between the electric static interaction and the magnetic static interaction.

The hydrodynamic forces acted on the particles are simply taken as the Stokes' drag:

$$\mathbf{F}_i^{\mathrm{hyd}} = -3\pi \eta_f \sigma \frac{d\mathbf{r}_i}{dt}. \tag{6}$$

A short-range repulsive force between two particles is used to account for the effect of the hard spheres [7–13],

$$F_{ij}^{\mathrm{rep}}(\mathbf{r}_{ij}) = F_0^{\mathrm{el}} \exp\left[\frac{-(r_{ij}/\sigma - 1)}{0.01}\right](-\mathbf{e}_r). \tag{7}$$

The random force $\mathbf{R}_i(t)$, which represents the net effect of collisions of solvent molecules on the particles, has a white noise distribution

$$\langle R_{i,\alpha} \rangle = 0, \quad \langle R_{i,\alpha}(0) R_{i,\beta}(t) \rangle = 6\pi K_B T \sigma \eta_f \delta_{\alpha\beta} \delta(t), \tag{8}$$

where K_B is the Boltzmann's constant, and T is the temperature. The average of $\mathbf{R}_i(t)$ over the simulation time step δt has a Gaussian distribution [9,10]. When both the electric and the magnetic fields are applied to the EMR system, the equation of motion of a particle is given by

$$m\frac{d^2\mathbf{r}_i}{dt^2} = \sum_{j \neq i} (\mathbf{F}_{ij}^{\mathrm{el}} + \mathbf{F}_{ij}^{\mathrm{mag}} + \mathbf{F}_{ij}^{\mathrm{rep}}) - 3\pi \eta_f \sigma \frac{d\mathbf{r}_i}{dt} + \mathbf{R}_i(t), \tag{9}$$

where m is the mass of the particle. Similar to the calculation of the local field, the summation in this equation is also evaluated within the cutoff separation of r_c. The variables can be rescaled as $t = t_0 t^*, F = F_0^{\mathrm{el}} F^*, r = \sigma r^*$, and $R = \Omega R^*$ with $t_0 = m/3\pi \eta_f \sigma$ and $\Omega = \sqrt{6\pi K_B T \sigma \eta_f / \delta t}$. The rescaled equation of motion can be written as [9,10]

$$\ddot{\mathbf{r}}_i^* = A(\mathbf{F}_i^* + B\mathbf{R}_i^*) - \dot{\mathbf{r}}^*, \tag{10}$$

where $A = F_0^{\mathrm{el}} t_0/3\pi \eta_f \sigma^2$, $B = \Omega/F_0^{\mathrm{el}}$, and $\mathbf{F}_i^* = \Sigma_{j \neq i}(\mathbf{F}_{ij}^{\mathrm{el}*} + \xi \mathbf{F}_{ij}^{\mathrm{mag}*} + \mathbf{F}_{ij}^{\mathrm{rep}*})$. A represents the ratio of the Reynolds number to the Mason number. B is a ratio of the Brownian force to the dipolar force. In Gulley and Tao's simulation work of an ER fluid, it is found that when $A \leqslant 10^{-3}$ the system is in the overdamped situation, i.e., $\ddot{\mathbf{r}}_i^* \approx 0$ [10]. In this case, Eq. (10) can be simplified to

$$\dot{\mathbf{r}}^* = A(\mathbf{F}_i^* + B\mathbf{R}_i^*). \tag{11}$$

By setting $t^* = t'^*/A$, the equation of motion now reduces to

$$d\mathbf{r}^*/dt'^* = \mathbf{F}_i^* + B\mathbf{R}_i^*, \tag{12}$$

which is independent of A. It means that in the overdamped situation the final structure is independent of A, but the time for the structure formation and transition is inversely proportional to A. When E_0 is on the order of kV/mm, A is estimated to be 10^{-4}–10^{-5} for the typical experimental parameters of ER and EMR fluids [6,14]. Therefore, instead of Eq. (10), we use Eq. (12) to study the structure evolution of the EMR system.

The parameter B characterizes the ratio of the Brownian force to the dipolar force. Though for a typical EMR fluid the dipolar energy is much stronger than the thermal energy, the thermal energy cannot be ignored for studying the ground-state structure of the fluid. In the simulations of ER and MR fluids, it had been found that when B is taken to be zero the systems are easily trapped in local-energy minimum states and end up in the complicated gel-like structures with no obvious lateral ordering [12,13]. For driving the systems from the local-energy minimum states to the global energy minimum states, a moderate B is usually needed. The Brownian force had been found to help the ER fluids to evolve into thick columns with bct lattice structure for a quite wide range of B [9,10]. In this paper, the thermal effect is also found to play an important role in the formation of the lattice structures in the EMR suspensions.

In adopting the local-field approximation to deal with the dipolar interactions between the particles, α and β, which represent the electric and magnetic polarization capabilities of the particles, respectively, are taken as the input parameters [7,8]. That enables us to study the effect of the material properties on the dynamic behavior of EMR suspensions in more details. In the present work, α and β are chosen to be the same value for convenience of discussion, although it is not easy to find an EMR material with both good ER and MR properties. The competition between the electric and magnetic interactions of the particles is then only determined by the parameter ξ which is taken to be 1 in most simulations, as we concentrate on studying the condition of compatible fields.

III. STRUCTURE FORMATION

The structure formation process in the EMR suspensions is investigated by applying the electric and magnetic fields simultaneously to the initial random configurations. The electric field is set along the z direction and the magnetic field is along the x direction. The initial configurations consist of N particles randomly dispersed in the three-dimensional (3D) simulation cell which has the scales of $8\sigma \times 8\sigma \times 8\sigma$ with periodic boundary conditions imposed in all three directions. The systems with $N = 108$, 256, and 365 have been studied, corresponding to the volume fraction of the particles $\Phi = 0.11$, 0.26, and 0.37, respectively. α and β are taken in the range of $0.4-1.0$ and B is in the range of $0-5.0$. After the fields are applied at $t'^* = 0$, the systems begin to evolve according to Eq. (12). This equation is integrated with a time step of $\delta t'^* \leqslant 10^{-3}$.

In simulations, we found that the structure evolution of the systems with different Φ are very similar in the initial stage. The combined electric and magnetic interactions between the particles draw them to form layer structures parallel to both fields. In each layer, the particles arrange into a two-dimensional close-packed hexagonal lattice with each particle in contact with six others. For the systems with larger Φ, the smaller separation between the layers makes them easily to combine with each other to form thicker sheetlike structures. The thick structures may relax into a 3D lattice with the help of the thermal fluctuations. But for the case of smaller Φ, only the single or double layers exist in the systems. It means that a relatively large Φ is needed for studying the formation of 3D lattice structure in the EMR suspensions.

The choice of the parameters α, β, and B can also influence the structure evolution of the suspensions obviously. Since the local-field effect has been considered in the simulations, the dipole moments on the particles, and thus the interaction forces between them are found to increase rapidly with the structuring of the particles due to the multibody polarization effects [7]. That makes the systems easily be trapped in the local-energy minimum states, and this effect is more obvious for the systems with larger α and β. At that time, larger Brownian force and longer relaxing time will be needed for the systems to relax into good lattice structures. The influence of the parameter B is found to be similar to that discussed in the simulation work of ER fluids [10]. When B is zero or very small, the final structure of the EMR systems are sensitive to the initial random configurations. For some initial states, the systems may develop into a good 3D crystal, but for others the systems will end up in a polycrystalline structure. When B is too large, the strong thermal fluctuations prevent the systems from forming any ordered structure. Our simulations found that for a moderate B in the range of 0.1–2.0, the Brownian force is helpful in driving the EMR systems from local-energy minimum states to global energy minimum states.

The structural evolution of an EMR system with $\Phi = 0.37, \alpha = \beta = 0.5$ under the conditions of $\xi = 1.0$ and $B = 1.0$ is shown in Fig. 1. The corresponding radial distribution function (RDF), which is defined as [12,15]

$$g_0(r^*) = \frac{\pi}{6\Phi N} \sum_i \sum_{j \neq i} \delta(r^* - r_{ij}^*), \tag{13}$$

is given in Fig. 2 in order to give a quantitative description of the structure character of the system. At $t'^* = 0$ [Fig. 1(a)], the particles are randomly distributed in the simulation cell. The radial distribution function of this structure [Fig. 2(a)] is consistent with the equilibrium RDF for a hard sphere liquid [12]. After application of the external fields, electric and magnetic dipoles are induced on the particles. The electric interaction forces between the particles lead them to have the tendency to form chain structures along the z direction, while the magnetic interaction forces lead to the tendency of forming chains along the x direction. If the effect of one field is much stronger than the other, chains or columns will still be formed along the dominant field direction. But when the two fields are compatible, the particles will rapidly arrange into

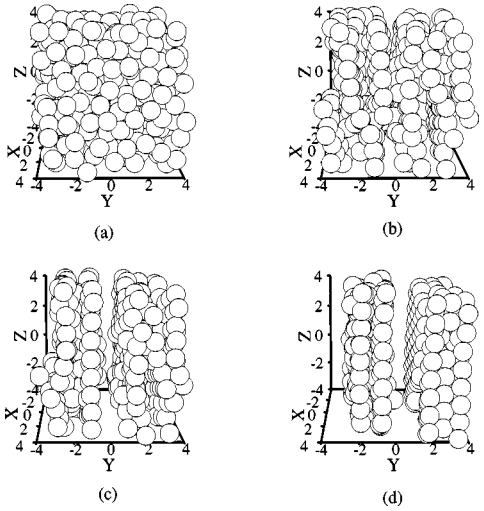

FIG. 1. The three-dimensional structure of an EMR system with $\Phi=0.37$ and $\alpha=\beta=0.5$ at different times: (a) $t'^*=0$, (b) $t'^*=2.8$, (c) $t'^*=8.0$, and (d) $t'^*=28$. The electric field is in the z direction and the magnetic field in the x direction. The conditions are $\xi=1.0$ and $B=1.0$. The unit is σ.

layer structures parallel to both fields due to the combined electric and magnetic forces. As can be seen in Fig. 1(b), several single layers have been formed in the system. The obvious growth and narrowing of the main peak at $r^*=1$ in the RDF of this structure [Fig. 2(b)], together with the appearance of the peaks at $r^*=\sqrt{3},2,\sqrt{7},3$, reflect the character of the 2D close-packed hexagonal lattice. The layer on the right-hand side of Fig. 1(b) is isolated and projected on the x-z plane in Fig. 3. It can be seen that the 2D hexagonal lattice has been roughly formed in this layer. The peaks in Fig. 2(b) correspond to the separations between particle 1 and its neighbors 2,3,4,5,6, separately. The vectors pointing from the center of particle 2 to particle 4 and from 2 to 3 can be considered as the primitive vectors for the 2D hexagonal lattice. The structures in other layers are very similar to Fig. 3, except that the directions of the primitive vectors may differ for different layers. Because the sixfold rotational axis of the 2D hexagonal lattice is perpendicular to the electric and magnetic dipole orientations, the dipolar energy of the lattice is invariant under the rotation around the sixfold axis

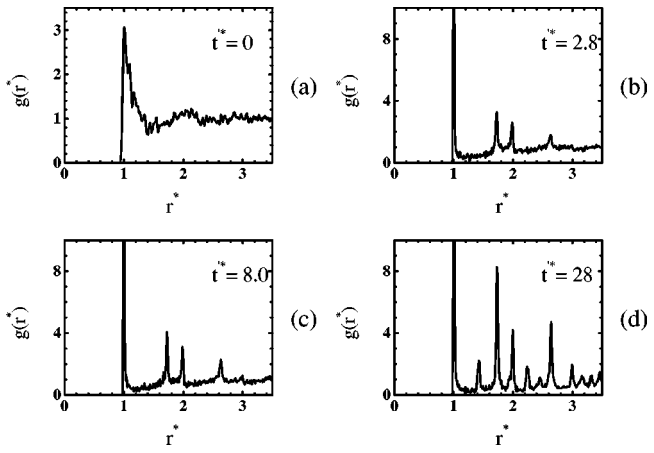

FIG. 2. The radial distribution functions of the particle configurations in Fig. 1.

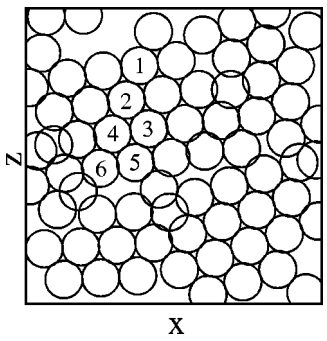

FIG. 3. The x-z plane projection of the layer on the right-hand side of Fig. 1(b). It can be seen that the two-dimensional hexagonal lattice has been roughly formed in this layer.

[5]. Thus under the compatible fields, there is no restriction for the arrangement direction of the 2D lattice in the x-z plane.

Since the interaction energy between the parallel layers is relatively weak and decays fast with the separation between them, the following structure evolution of the system depends on the volume fraction of the particles obviously. When Φ is small, there are only a few single layers formed in the system. The larger separation makes it difficult for the layers to combine with each other. The layers remain isolated. The structure evolution of the system will stop after the internal structure in each layer has reached the well-arranged 2D hexagonal lattice. This case has been observed evidently in the simulations with $\Phi=0.11$. When Φ is larger, the interaction energy between the layers increases due to the smaller separation. The electric and magnetic attractive forces draw the layers combine together to form thick sheetlike structures. Figure 1(c) shows such a case, where three single layers combine with each other on the right side and two others combine on the left. The RDF of this structure is given in Fig. 2(c). No new peak appears in this figure when compared with Fig. 2(b). It means that there is still no lateral ordering in the y direction. The growth of the existed peaks indicate that the 2D hexagonal lattices in the layers become more complete. If B is taken to be zero or very small, the structure evolution of the EMR system usually end up in such a polycrystalline state, because it is difficult for the particles to leave their local-energy minimum positions. The final structure is sensitive to the initial random state in this case. But when a moderate B is applied, the thermal fluctuations can drive the system to good lattice structure. This can be seen clearly on the right side of Fig. 1(d), where the three combined layers have relaxed into a 3D close-packed structure after a long enough relaxing time. The packing of the two other layers is not so good, because there is a large rotation angle between the two 2D hexagonal lattices. In the RDF of the system [Fig. 2(d)], the formation of the 3D close-packed structure is reflected by the obvious growth of the peaks corresponding to the 2D hexagonal lattice and the appearance of the new peaks at $r^*=\sqrt{2},\sqrt{5},\sqrt{6}$ which correspond to the separations between the particles in two close-packed single layers.

The close-packing of the 2D hexagonal layers can form two 3D lattices [16]. The $ABCABC\cdots$ series is the fcc lattice and the $ABAB\cdots$ series is the hcp lattice. If we suppose that the 2D close-packed layers are in the x-z plane

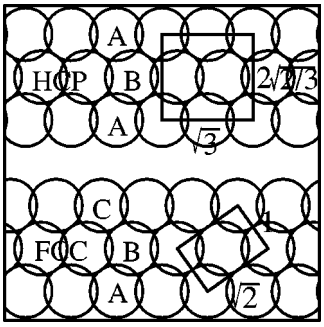

FIG. 4. Projections of the hexagonal close-packed (hcp) and face-centered cubic (fcc) lattices on the plane perpendicular to their 2D hexagonal layers. The projected structures can be represented by two 2D crystals which are depicted with the two rectangular frames. The unit is σ.

with one of their primitive vectors along the z direction, the primitive vectors for the 3D fcc lattice can be written as $\mathbf{a}_1^{\mathrm{fcc}}=\sigma\mathbf{z}^0$, $\mathbf{a}_2^{\mathrm{fcc}}=\sigma/2(\sqrt{3}\mathbf{x}^0+\mathbf{z}^0)$, and $\mathbf{a}_3^{\mathrm{fcc}}=\sigma/2(1/\sqrt{3}\mathbf{x}^0+2\sqrt{2/3}\mathbf{y}^0+\mathbf{z}^0)$. The two former vectors determine the particle arrangement in the 2D hexagonal lattices and the third one gives the lateral order of the 3D fcc lattice. For the hcp lattice, there are two particles in one primitive cell. One particle is in the A layers, the primitive vectors for which are $\mathbf{a}_1^{\mathrm{hcp}A}=\sigma\mathbf{z}^0$, $\mathbf{a}_2^{\mathrm{hcp}A}=\sigma/2(\sqrt{3}\mathbf{x}^0+\mathbf{z}^0)$ and $\mathbf{a}_3^{\mathrm{hcp}A}=2\sqrt{2/3}\sigma\mathbf{y}^0$. The other is in the B layers, which has a displacement of $\mathbf{r}_0^{\mathrm{hcp}B}=1/3\mathbf{a}_1^{\mathrm{hcp}A}+1/3\mathbf{a}_2^{\mathrm{hcp}A}+1/2\mathbf{a}_3^{\mathrm{hcp}A}$ with that in A. The projections of the two 3D lattices on the plane perpendicular to the 2D layers are shown in Fig. 4 and described by two 2D crystals there. The Bravais vectors of the 2D crystals are $\mathbf{a}_1=\sigma\mathbf{a}_1^0$ and $\mathbf{a}_2=\sqrt{2}\sigma\mathbf{a}_2^0$ for fcc, and $\mathbf{a}_1=\sqrt{3}\sigma\mathbf{a}_1^0$ and $\mathbf{a}_2=2\sqrt{2/3}\sigma\mathbf{a}_2^0$ for hcp. In the RDFs, both fcc and hcp have peaks at $r^*=1,\sqrt{2},\sqrt{3},2,\sqrt{5},\sqrt{6},\sqrt{7},3,\ldots$ which reflect the close-packing of the 2D hexagonal layers. But there are still peaks at $r^*=\sqrt{8/3},\sqrt{11/3}$, and $\sqrt{17/3}$ for hcp that correspond to the relative positions between the particles in two neighboring A layers or two B layers. As referred in Sec. II, when the 2D layers are parallel to the plane determined by the crossed electric and magnetic fields, the dipolar energy difference between the hcp and fcc structures is very small and compatible to the thermal energy at room temperature. Thus the 3D close-packed structure which is formed in the EMR system with the help of the thermal fluctuations may be a hcp lattice, a fcc lattice, or, more likely, a hcp-fcc mixed structure [5].

The quantitative analysis of the lattice character of the 3D structure can be obtained from its order parameters which are defined as [9,10]

$$\rho_j^{\mathrm{lattice}}=\frac{1}{N}\sum_{i=1}^{N}\exp(i\mathbf{b}_j^{\mathrm{lattice}}\cdot\mathbf{r}_i)\quad(j=1,2,3),\qquad(14)$$

where $\mathbf{b}_j^{\mathrm{lattice}}$ are the reciprocal lattice vectors of the ideal 3D periodic structures. For the fcc lattice, we have $\mathbf{b}_1^{\mathrm{fcc}}=2\pi/\sigma(-1/\sqrt{3}\mathbf{x}^0-1/\sqrt{6}\mathbf{y}^0+\mathbf{z}^0)$, $\mathbf{b}_2^{\mathrm{fcc}}=2\pi/\sigma(2/\sqrt{3}\mathbf{x}^0-1/\sqrt{6}\mathbf{y}^0)$ and $\mathbf{b}_3^{\mathrm{fcc}}=2\pi/\sigma(\sqrt{3/2}\mathbf{y}^0)$. For the hcp structure, the reciprocal vectors about $\mathbf{a}_j^{\mathrm{hcp}A}$ are $\mathbf{b}_1^{\mathrm{hcp}A}=2\pi/\sigma(-1/\sqrt{3}\mathbf{x}^0+\mathbf{z}^0)$, $\mathbf{b}_2^{\mathrm{hcp}A}=2\pi/\sigma(2/\sqrt{3}\mathbf{x}^0)$ and $\mathbf{b}_3^{\mathrm{hcp}A}=\pi/\sigma(\sqrt{3/2}\mathbf{y}^0)$, which can also be used to calculate $\rho_j^{\mathrm{hcp}B}$ by

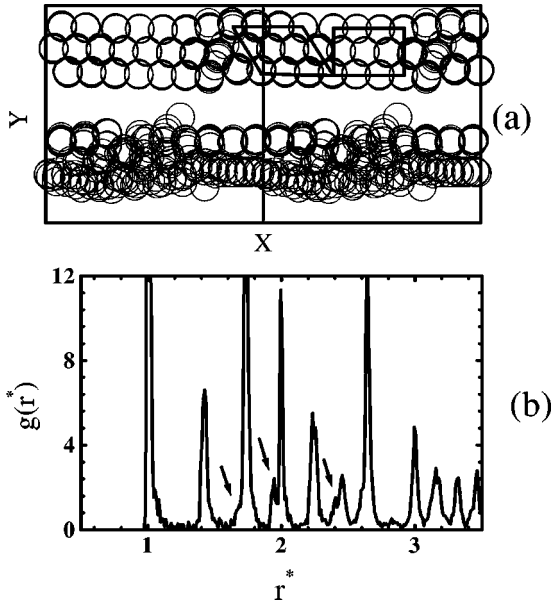

FIG. 5. (a) The simulation cell in Fig. 1(d) is repeated in the x direction and projected on the x-y plane to show the periodic structures more clearly. There is a fcc structure in the parallelogram frame and a hcp structure in the rectangular frame. (b) Radial distribution function of the structure in the upper part of (a). The arrows point out the special peaks corresponding to the hcp structure. This result reflects that the structure in the upper part of (a) is a hcp-fcc mixed structure.

replacing $\mathbf{r}_i$ with $\mathbf{r}_i-\mathbf{r}_0^{\mathrm{hcp}B}$ in Eq. (14). If the structure formed in the EMR system is a complete fcc (or hcp) structure, the order parameters ρ_j^{fcc} (or $\rho_j^{\mathrm{hcp}A}$ and $\rho_j^{\mathrm{hcp}B}$) should equal 1. On the contrary, they will be zero if the system is in a random state. The calculations are carried out to the 3D close-packed structure on the right side of Fig. 1(d), in which the coordinate rotation is used for getting the largest $\Pi_{j=1,3}\rho_j$. The order parameters about fcc lattice are obtained to be $\rho_j^{\mathrm{fcc}}=5.49$, 7.69, and 5.70, respectively, while that about hcp are $\rho_j^{\mathrm{hcp}A}=7.78,7.46,7.36$ and $\rho_j^{\mathrm{hcp}B}=8.03,8.73,9.18$, separately. The relative large values of $\rho_j^{\mathrm{hcp}B}$ reflect the close-packing character of the layers, but the smaller values of ρ_j^{fcc} and $\rho_j^{\mathrm{hcp}A}$ imply that the 3D structure in Fig. 1(d) is not a complete fcc or hcp lattice. This is clarified in Fig. 5(a) where the simulation cell is repeated periodically in the x direction and projected on the x-y plane. When comparing with Fig. 4, we can see that the 3D close-packed structure is just a mixed hcp-fcc structure in that the hcp and fcc lattices are nearly of the same proportion. For the structure in the parallelogram frame, the order parameters about fcc are $\rho_j^{\mathrm{fcc}}=9.92$, 9.85, and 9.47, respectively. For that in the rectangular frame, the parameters about hcp are $\rho_j^{\mathrm{hcp}A}=9.97,9.99,9.90$ and $\rho_j^{\mathrm{hcp}B}=9.96,9.97,9.92$, separately. When the calculation of the RDF is confined to this mixed structure, the result [Fig. 5(b)] show that the common characteristic peaks of the hcp and fcc become very obvious and even the special peaks at $\sqrt{8/3}$, $\sqrt{11/3}$, and $\sqrt{17/3}$ for the hcp lattice can also be found. The formation of this mixed structure is because there is a gap with width of $\sigma/\sqrt{3}$ in the x direction in the top layer. This distance is just the relative lateral shift between the A layer and the C layer of the fcc lattice as shown in Fig.

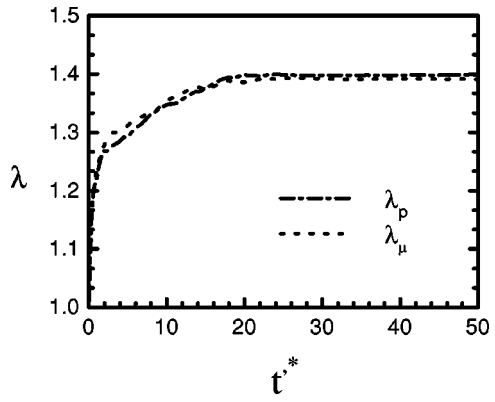

FIG. 6. Time variation of the mean-square electric and magnetic dipole strength of the particles in the system studied in Fig. 1. The simultaneous growth of λ_p and λ_m indicates the symmetrical development of the structure in the electric and magnetic field directions.

4. Without this gap, the top layer can be a complete *C* (or *A*) layer, and the three layers will form a complete fcc (or hcp) lattice.

Figure 6 shows the time variation of the mean-square electric and magnetic dipole strengths on the particles which are defined as [7]

$$\lambda_p(t'^*)=\frac{1}{N}\sum_i^N p_i^{*2}(t'^*),$$
$$\lambda_m(t'^*)=\frac{1}{N}\sum_i^N m_i^{*2}(t'^*). \tag{15}$$

Due to the mutual polarization effect, the dipole strengths on the particles increase obviously with the formation of structures, see Eqs. (1)–(3) and (5). The time variation of the parameters λ_p and λ_m can thus be used to analyze the time scale of the structure evolution in the EMR system. The simultaneous growth of λ_p and λ_m in Fig. 6 reflects the symmetrical development of the structures in the *x* and *z* directions, i.e., the formation of the layer or sheetlike structures. The structuring process in the EMR system can be divided into two regimes. In the first regime, the single layers are formed rapidly. The dimensionless time t'^* for this period is less than 3 in Fig. 6. In the following regime, the single layers combine with each other to form thicker sheetlike structures and the thicker structures relax into 3D close-packed structures with the help of the thermal fluctuations. The second process is much slower than the first one. It takes dimensionless time of about $t'^*\sim 20$ for the system to build up lateral ordering in the *y* direction. After that there is no obvious structure variation because the system is approaching to its global energy minimum state. Figure 1(d) is taken at this time. If the experimental parameters are available for calculating t_0 and *A*, the real time scale for the structure evolution of the EMR system can be obtained directly from the dimensionless time discussed above.

The formation of the 3D close-packed structures has been found for nearly all of the initial random configurations we studied with $\Phi=0.37$ when a moderate *B* is applied. Some of them are complete fcc or hcp structures, while others are the mixed fcc-hcp structures. This originates from the different stacking form of the 2D hexagonal layers in the *y* direction. If the layers stack in an order of $ABCABC\cdots$ (or $ABAB\cdots$), we got a fcc (or hcp) structure. But in most cases the stacking of the layers are in random order and the 2D layers themselves are not so complete, thus the mixed fcc-hcp structures are obtained more easily. In Fig. 1(d), the result is due to the defect in one layer. The layers are also found to stack in the order of *ABCB* in simulations. For the former three layers, it is a fcc structure. While for the latter three ones, it is a hcp. Since the primitive vectors of the 2D hexagonal layers can arrange in different directions in the *x*-*z* plane, the lattice axes of the formed 3D close-packed structures are also found to orient differently with respect to the electric and magnetic fields. The details of the final structures depend on the initial configurations, the thermal fluctuations as well as the polarization parameters α and β of the particles. The different 3D close-packed structures obtained in simulations are consistent with the theoretical predictions for the lattice structures formed in EMR systems under the compatible fields [5].

IV. STRUCTURE TRANSITION

For studying the structure transition in EMR systems, the electric field is supposed to be applied at first to induce the bct columns along the *z* direction. The magnetic field is then applied in the perpendicular direction [6]. Since the formation of the bct structures in ER fluids has been studied in details by the theoretical and simulation methods [9,10], we will not discuss it in this paper. The simulations are thus started with the preset cylindrical bct columns with their fourfold rotational axis along the electric field direction. The columns have the diameter ranging from 7σ to 9σ and their three conventional Bravais vectors are taken to be $\mathbf{a}=(\sqrt{6}\sigma/2)\mathbf{x}^0$, $\mathbf{b}=(\sqrt{6}\sigma/2)\mathbf{y}^0$, and $\mathbf{c}=\sigma\mathbf{z}^0$ [6]. With the periodic boundary conditions applied in three directions, the columns are supposed to be infinitely long in the *z* direction and arrange into a two-dimensional square lattice in the *x*-*y* plane. The electric field is assumed to be applied for all the time, and the magnetic field is switched on at $t'^*=0$ in the *x* direction, i.e., **a** axis of the bct lattice.

Figure 7 shows the structure transition in an EMR system consisting of cylindrical bct columns with a diameter of 8σ and polarization capabilities $\alpha=\beta=0.5$. The scales of the simulation cell in the *x*-*y* plane is $10\sigma\times 10\sigma$ which corresponds to the volume fraction of the particles $\Phi=0.36$. ξ is set to be 1 for the compatible fields and *B* is taken to be zero. It has been found that the effect of the thermal fluctuations are relatively weak when the initial state is the complete lattice structure. For a quite wide range of *B*, the simulation results are found to be essentially the same in this case.

If only the electric field is applied, the suspension works as an ER fluid. So the initial bct columns [Fig. 7(a)] are very stable even under relatively large thermal fluctuations. However, when the magnetic field is switched on, the bct structure is no longer the ground state for the system. The demagnetization effect favors the lattice deformation of a/c increasing [6], resulting in the stretch of the columns along the *x* direction. The lattice vector **a** increases, while vector **b** decreases. The lattice vector **c** keeps invariant and the chain structures stay intact in the *z* direction in the whole process

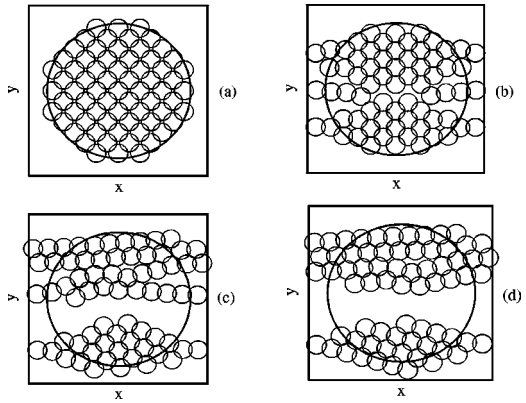

FIG. 7. The x-y plane projections of an EMR system with cylindrical bct columns as its initial state at (a) $t'^*=0$, (b) $t'^*=1.5$, (c) $t'^*=9.5$, and (d) $t'^*=20$. The c axis of the initial bct columns is in the electric field (z) direction. The magnetic field is applied along a axis of the bct columns (x direction). The diameter of the initial column is 8σ. The scales of the simulation cell is $10\sigma \times 10\sigma$ in the x-y plane, which gives to the volume fraction of the particles $\Phi=0.36$. Here $\alpha=\beta=0.5$, $\xi=1.0$, and $B=0$.

of the structure transition. After a very short time, **a** turns to be $\sqrt{2}\sigma\mathbf{x}^0$ and **b** to $\sigma\mathbf{y}^0$, as shown in Fig. 7(b). Due to the rapid decrease of **b**, the bct column is found to break into two parts in the y direction. In each part, **a** and **b** construct a 2D rectangular lattice with $a/b=\sqrt{2}$ in the x-y plane, implying the formation of the fcc structure. The order parameters about fcc for the system are $\rho_j^{\mathrm{fcc}}=9.28,\ 7.40$, and 7.44, respectively. The relative small values of ρ_j^{fcc} result from the particles at the outer parts of the columns in the y direction. At this time, the 2D hexagonal layers are at an angle of about 35.3° with respect to the x-z plane, while this angle is 45° for the bct structure in the initial configuration. The rotation of the close-packed layers toward the magnetic field direction is understood as the requirement for the EMR system to reach the global energy minimum state. Although our simulation model adopts the induced magnetic moment, instead of the permanent moment, to describe the magnetic properties of the particles, the simulated dynamic process of the bct-fcc structural transition is found to agree well with the experimental observations as well as the theoretical explanation in Ref. [6].

We have also studied the effect of the magnetic field strength on the structural transition by changing the parameter ξ from 0 to 1. The application of the magnetic field is always found to induce the deformation of the bct columns along the x direction. When ξ is up to 0.5 the bct to fcc structural transition can be observed obviously. While for $\xi<0.5$, the magnetic field is relatively weak and cannot stretch the columns to a structure with $a/b=\sqrt{2}$ completely. In that case it is found that the columns usually develop into a polycrystalline structure with local fcc structures and local bct structures. This result is qualitatively consistent with that observed in experiments as well [6], though the material properties studied in our simulations differ from those in experiments. We have changed the diameter of the columns, the scales of the simulation cell and the thermal fluctuations in simulations. The bct to fcc transition has been found for all the simulations when ξ is large enough. If the external fields are removed at this time and the structures are frozen by physical or chemical methods, the complete fcc mesocrystals may be obtained. However, if the fields are still applied, our simulations found that the structure will keep on evolving at a relatively slow speed after the structure transition. This may be understood as the result of the obvious demagnetization field effect at the rough surface of the deformed column structures as shown in Fig. 7(b).

The subsequent structure evolution of the system depends on the volume fraction of the particles Φ obviously. Here Φ is determined by the diameter of the initial bct columns and the scales of the simulation cell in the x-y plane. When Φ is smaller, the larger separation between the columns gives them enough space to relax. Following the bct to fcc transition, the structures keep on stretching along the x direction until all the particles arrange into 2D close-packed layers parallel to both fields. Because of the smaller Φ, only the single or double layer structures are obtained under this condition. In the extreme case that there is only one bct column in the system, i.e., no periodic boundary conditions are imposed, the structure is found to develop into several single layers rapidly. On the other hand, when Φ is larger, the columns touch their neighbors in the x direction soon after the deformation, see Fig. 7(b). The relaxation of the structures in the limited space [Fig. 7(c)] leads to the formation of thicker sheetlike structures. It can be seen in Fig. 7(d) that two 3D close-packed structures have been formed in the system. The structure in the upper part is a hcp lattice. Its order parameters about hcp are $\rho_j^{\mathrm{hcp}A}=5.08,9.59,9.48$ and $\rho_j^{\mathrm{hcp}B}=6.21,9.04,9.55$, separately, considering the deformation of the two lower layers. The structure in the lower part of Fig. 7(d) is a fcc lattice with order parameters of $\rho_j^{\mathrm{fcc}}=9.97,\ 9.81$, and 9.68, respectively. The only difference between these lattice structures and those in Fig. 4 is that the orientation of the 2D hexagonal layers is at an angle with the x-z plane in this case. As discussed above, this angle will decrease with the increase of the separation between the initial bct columns. In simulations, it has been found that when Φ is not smaller than 0.3 the structures can always relax into the 3D close-packed lattices. The details of the 3D lattices depend on the initial configurations and the competition between the magnetic and the electric fields. In Fig. 7(d), the hcp and fcc structures are separate. The mixed fcc-hcp structure has also been found. For example, we have increased the simulation cell in Fig. 7 to $11\sigma\times11\sigma$ and fixed other conditions. In the upper part of the final configuration, we find four single layers close-packing in an order of $ABCB$. This is the mixed structure as mentioned in Sec. III. Thus the structure transition of the EMR system can also be divided into two steps. In the first step, the bct structures transform to the fcc structures with $a/c=\sqrt{2}$. The fcc structures then relax into the 3D close-packed structures with their 2D hexagonal layers turning toward the x-z plane as far as possible in the second step. The final structures may be the fcc, the hcp, or, more likely, the fcc-hcp mixed structures.

V. CONCLUSION

In this paper, the molecular dynamic simulation method has been used to study the structural formation and transition in EMR fluids under the compatible electric and magnetic

fields. The structural formation process is investigated by applying the fields crossed and simultaneously to the initial random configuration. It has been found that the particles at first form 2D hexagonal layers parallel to both fields. When the volume fraction of the particles is large enough, the layers combine each other to form thicker sheetlike structures. The thick structures further relax into 3D close-packed lattices with the help of thermal fluctuations. Since the dipolar energy difference between the fcc and hcp lattices is very small, the final structures may be the fcc, the hcp, or, most probably, the fcc-hcp mixed structures, depending on the initial configurations and the thermal fluctuations. For studying the structural transition observed in experiments [6], the cylindrical bct columns are supposed to be formed at first with their c axis along the electric field direction. The magnetic field is then applied along the a axis of the bct structures. When the magnetic field is strong enough, the structure transition of the EMR system is found to be composed of two steps. In the first step, the bct columns transform to fcc structures with $a/c=\sqrt{2}$ due to the demagnetization effect. The structures further relax into 3D close-packed structures with their 2D hexagonal layers turning toward the plane determined by both fields as far as possible in the second step. The final structures are also found to be the fcc, hcp, or fcc-hcp mixed structures. The simulation results are consistent with the theoretical and experimental results well [5,6].

ACKNOWLEDGMENTS

This work was supported by the National Science Foundation of China through Grant No. 19774019. Z. Lin was also supported by NSFC Grant No. 19834070.

[1] J. D. Carlson, in *Electrorheological Fluids, Magnetorheological Suspensions and Associated Technology*, edited by W. A. Bullough (World Scientific, Singapore, 1996), p. 20.
[2] W. I. Kordonsky, S. R. Gorodkin, and E. V. Medvedeva, in *Electrorheological Fluids*, edited by R. Tao and G. D. Roy (World Scientific, Singapore, 1994), p. 22.
[3] K. Koyama, in *Electrorheological Fluids, Magnetorheological Suspensions and Associated Technology* (Ref. [1]), p. 245.
[4] K. Minagawa, T. Watanabe, K. Koyama, and M. Sasaki, Langmuir **10**, 3926 (1994).
[5] R. Tao and Qi Jiang, Phys. Rev. E **57**, 5761 (1998).
[6] W. Wen, N. Wang, H. Ma, Z. Lin, W. Y. Tam, C. T. Chan, and P. Sheng, Phys. Rev. Lett. **82**, 4248 (1999).
[7] Z. W. Wang, Z. F. Lin, and R. B. Tao, Int. J. Mod. Phys. B **10**, 1153 (1996).
[8] Z. W. Wang, Z. F. Lin, H. P. Fang, and R. B. Tao, J. Phys. D **30**, 1265 (1997).
[9] R. Tao and Qi Jiang, Phys. Rev. Lett. **73**, 205 (1994).
[10] G. L. Gulley and R. Tao, Phys. Rev. E **56**, 4328 (1997).
[11] D. J. Klingenberg, F. Van Swol, and C. F. Zukoski, J. Chem. Phys. **91**, 7888 (1989).
[12] K. C. Hass, Phys. Rev. E **47**, 3362 (1993).
[13] M. Mohebi, N. Jamasbi, and J. Liu, Phys. Rev. E **54**, 5407 (1996).
[14] For example, see *Electrorheological Fluids*, edited by R. Tao and G. D. Roy (World Scientific, Singapore, 1994); *Electrorheological Fluids, Magnetorheological Suspensions and Associated Technology* (Ref. [1]).
[15] M. P. Allen and D. J. Tildesley, *Computer Simulation of Liquids* (Clarendon, Oxford, 1989).
[16] R. Tao and J. M. Sun, Phys. Rev. Lett. **67**, 398 (1991).